Tripterygium glycoside ameliorates kidney injury in diabetic rats by regulating the PI3K/Akt signaling pathway

Dandan HOU[1], Sainan SHANG[1], Juan LV[1], Shuling WANG[1]*

Abstract

To discuss protective effect of Tripterygium Glycoside (TG) on renal injury in diabetic rats and preliminary exploration of its mechanism. The rats were divided into Normal, Model, Low, Middle and High groups. Measuring FBG, TG, TC, HDL-C, BUN and Scr concentration by ELISA assay; using coomassie brilliant blue method to measure 24 h Urine protein. Measuring Kidney index; using HE staining to observation renal histomorphological changes; The ultrastructural changes of renal tissue were observed by transmission electron microscope; TUNEL staining was used to detect the apoptosis of rat renal cells; using WB assay to evaluate PTEN, PI3K, Akt, Bcl-2, Bax and caspase-3 expression. Compared with Normal group, FBG, TG and TC concentrations significantly increased and HDL-C concentration significantly decreased (P < 0.001); BUN, Scr and 24 h Urine protein significantly up-regulated (P < 0.001); Kidney weight and KI significantly down-regulated; Kidney injury score and apoptosis cell number significantly increased (P < 0.001) with PTEN, Bcl-2 protein downregulation and PI3K, Akt, Bax and caspase-3 protein expression significantly up-regulation in Model group (P < 0.001). With TG supplement, the kidney injury significantly improved. TG improved diabetic induced kidney injury via PI3K/Akt pathway in vivo.

Keywords: TG; diabetic; kindy injury; PI3K.

Practical Application: TG had improved diabetic induced kidney injury.

1 Introduction

Diabetes is a common clinical chronic disease, which, with a reported incidence of 9.7%, has imposed an increasing burden on the global population as the third most hazardous condition following cardio/cerebrovascular diseases and cancers (Giugliano et al., 2021). Patients with diabetes are susceptible to microvascular complications (e.g., diabetic nephropathy) because their blood glucose levels are persistently high. Considering the insidious onset and lengthy disease course, these microvascular complications can end up causing end-stage kidney failure. Therefore, it is imperative to clarify the underlying pathogenesis and implement effective prevention and control measures against diabetes (Izzo et al., 2021). For diabetic nephropathy, the phosphatidylinositol 3-kinase / protein kinase B (PI3K/Akt) signaling pathway is a key player in signal transduction, while excessive activation of the PI3K/Akt signaling pathway can promote the development and progression of diabetic nephropathy (Lu et al., 2019). Phosphatase and tensin homolog deleted on chromosome 10 (PTEN) is found to suppress the activation of the PI3K/Akt signaling pathway and thereby inhibit the development and progression of diabetic nephropathy (Xing et al., 2015). Since 1970s, tripterygium glycoside (TPG) has been identified as a useful traditional Chinese medicine of potent anti-inflammatory and immunosuppressive properties and has attracted strong interest from domestic and foreign researchers as it produces good therapeutic effect on rheumatoid arthritis, lupus and other autoimmune disorders and shows satisfactory

efficacy in clinical treatments (Su et al., 2013). However, it has not yet been clarified the efficacy and mechanism of action of TPG in treating diabetes-induced kidney injury. In this study, a rat model of diabetes-induced kidney injury was administered with TPG as drug intervention to observe the effect of TPG on the PI3K/Akt signaling pathway and investigate the mechanism of action of TPG in treating diabetic nephropathy.

2 Materials and methods

2.1 Experiment animals

Male SPF Sprague-Dawley rats (body weight: 0.2-0.4 kg; age: 8 weeks; certificate number: SYXK (J) 2017-0001) were provided by the Laboratory Animal Center of Hebei North University. To prepare for modeling, all rats underwent adaptive feeding (free intake of deionized water and food) for 1 week in the same environment where the indoor temperature ranged between 22 °C and 25 °C and the relative humidity was 40-60%.

2.2 Reagents and instruments

Streptozotocin (STZ, Amresco, USA, Batch No.: 170223); blood urea nitrogen (BUN), serum creatinine (SCr) Detection Kits (Nanjing Jiancheng Bioengineering Institute, China, Batch No.: C013-2 and C011-2); Hematoxylin & Eosin (HE) Stain Kit, TUNEL Assay Kit, and RIPA lysis buffer (Beyotime

Biotechnology Institute, China, Batch No.: C0105, C1086, and P0013B); glutaraldehyde (GA) and bicinchoninic acid (BCA) protein assay kits (Beijing Solarbio Science & Technology Co., Ltd., China, Batch No.: DF0157 and PC0020); uranyl acetate (UA) (Shenzhen Excellent Biotech Co., Ltd., China, Batch No.: 541093); lead citrate (LC) (Jinjinle Chemical Co., Ltd., China, Batch No.: 512265); rat anti-PTEN, PI3K, p-Akt, and Akt antibodies (CST, USA, Batch No.: 9556, 13666, 12694, and 2920); B-cell lymphoma 2 (Bcl-2), Bcl-2-associated X protein (Bax), caspase-3, β-actin, horseradish peroxidase (HRP)-labeled IgG antibody (Abcam, USA, Batch No.: ab692, ab232479, ab179517, ab156302, and ab205719); E-6 blood glucose (BG) meter (Roche, USA); DxC automatic biochemistry analyzer (Beckman Coulter, USA); CKX53 inverted microscope, and IXTI-12FL/PH fluorescence microscope (Olympus, Japan); transmission electron microscope (TEM, HITACHI, Japan); 1658001 vertical electrophoresis system, 1703930 MiniTrans-Blot cell small transfer tank, and ChemiDoc XRS system (Bio-Rad, USA).

2.3 Modeling for diabetes-induced kidney injury

Before modeling, rat tail venous blood samples were collected and BG levels were determined to range between 4 to 6 mmol/L. 9 rats were randomly chosen to form the normal group fed on a normal diet. The rest 51 rats were used for modeling after fasting for 12 h, during which they were allowed to drink as normal. Then, 60 mg/kg STZ citric acid buffer solution was injected intraperitoneally 72 h before determination of their BG levels using corresponding tail venous blood samples. The diabetic rat model was established successfully when the fasting blood glucose (FBG) level exceeded 16.7 mmol/L (Malik et al., 2017); in the meantime, the normal group received citric acid buffer solution in the equivalent volume via intraperitoneal injection. The rats were fed for another 3 d before 24-h urine collection, and the diabetic rat model of kidney injury was constructed successfully when the urine protein (UP) level was >30 mg (Lei et al., 2018). A total of 6 rats died in this process, indicating a success rate was 88.24%.

2.4 Route of administration and grouping

Eventually, the normal group had 9 rats, while another 36 rats were assigned to a diabetes-induced kidney injury group (i.e., the model group), and low-, medium-, and high-dose TPG groups (LDTPG: 1 mg/kg, MDTPG: 2 mg/kg, and HDTPG: 8 mg/kg) (Wan et al., 2013), with each group having 9 rats, respectively; the normal group and the model group were given equal volumes of distilled water on a daily basis. The rats were treated for 8 weeks.

2.5 Sample collection and outcome measures

Determination of serum levels of FBG, triacylglycerol (TG), total cholesterol (TC), and high-density lipoprotein cholesterol (HDL-C). Following the last administration, tail venous blood was collected from each rat to test the FBG level using a glucometer and measure the TG, HDL-C, and TC levels using an automatic biochemistry analyzer.

2.6 BUN and SCr detection

Each blood sample was centrifuged at 3000 g/min for 5 min to isolate serum for determination of the BUN and SCr levels using the ELISA kit as instructed by the manufacturer.

2.7 24-h UP measurement

Subsequent to 24-h urine collection, the UP level was measured with the Coomassie Brilliant Blue G-250 method.

2.8 Sample collection

Each rat was weighed after tail venous blood collection and was killed after anesthesia to harvest and weigh the left kidney tissue, which was evenly divided into two parts for refrigeration at -80 °C and fixation in 4% paraformaldehyde (PFA), respectively.

2.9 Pathomorphology of kidney

Paraffin sectioning, dewaxing, and hydration were performed in the routine manner to prepare for staining with the H&E Stain Kit, and the sections were placed under a microscope to observe changes in the morphological structures of kidney tissue. Scoring of tubular injury was conducted via semi-quantification analysis using Paller's method (Jablonski et al., 1983) to evaluate cell degeneration, dilation, necrosis, and granular degeneration.

2.10 Ultrastructure of kidney tissue under TEM

The harvested kidney tissue was washed with 2.5% GA and fixed in phosphate buffered saline (PBS) at 4 °C for 2 h, followed by rinsing and addition of acetone. After standing at room temperature for 20 min, the kidney tissue was embedded in epoxy resin to prepare 0.06 μm ultra-thin sections. Then, the UA-LC staining procedure was performed, and the stained sections were placed under a TEM to observe the ultrastructure of the kidney tissue.

2.11 Observation of cell apoptosis in kidney tissue by TUNEL staining

Staining of kidney tissue sections was performed as instructed using the TUNEL assay kit, while DAPI (4′,6-diamidino-2-phenylindole) staining was conducted to identify cell nuclei. Subsequently, a fluorescence microscope was employed to observe cell apoptosis in the kidney tissue. The ImageProPlus 6.0 software was used for quantitative analysis of cell counts in the kidney tissue.

2.12 Determination of PTEN, PI3K, p-Akt, Bcl-2, Bax, and caspase-3 protein expression in kidney tissue by Western blotting (WB)

After grinding, the kidney tissue was added with RIPA lysis buffer for total protein (TP) extraction, and the TP concentration was determined using the BCA method. Sodium dodecyl sulfate polyacrylamide gel electrophoresis (SDS-PAGE) was performed to isolate target proteins, followed by membrane transfer, blocking, addition of primary PTEN, PI3K, p-Akt, Bcl-2,

Bax, and caspase-3 antibodies (diluted at 1:500) for membrane incubation overnight at 4 °C, and incubation with the HRP-labeled IgG secondary antibody at room temperature for 2 h. After washing, exposure, and development, the ChemiDoc XRS system was used for automated image capture and observation of proteins, and the ImageProPlus 6.0 software was for quantitative analysis of protein expression.

2.13 Statistical analysis

All data were expressed in the form of "mean ± standard deviation (m±sd)". Intergroup comparison was examined by one-way analysis of variance (ANOVA), and P <0.05 indicated a difference of statistical significance. The software SPSS19.0 was used for statistical analysis.

3 Results

3.1 Intergroup comparison of BG and blood lipid levels

Compared with the normal group, the model group exhibited significant increases in the FBG, TG, and TC levels and a marked decrease in the HDL-C level (P < 0.001, respectively, Table 1). Compared with the model group, the LDTPG, MDTPG, and HDTPG groups experienced substantial reductions in the FBG, TG, and TC levels and a considerable elevation in the HDL-C level (P < 0.05, respectively, Table 1). There were significant differences among the LDTPG, MDTPG, and HDTPG groups in the FBG, TG, TC, and HDL-C levels (P <0.05, respectively, Table 1).

3.2 Intergroup comparison of levels of urinary metabolic markers

The BUN, SCr, and 24-h UP levels were significantly increased in the model group as compared with the normal group

(P < 0.001, respectively, Table 2). The BUN, SCr, and 24-h UP levels were significantly reduced in the LDTPG, MDTPG, and HDTPG groups when compared with the model group (P < 0.05, respectively, Table 2); the differences among the LDTPG, MDTPG, and HDTPG groups in the BUN, SCr, and 24-h UP levels were statistically significant (P < 0.05, respectively, Table 2).

3.3 Effects of TPG on Kidney weight (Kw), Body weight (Bw), and Kidney index (KI)

In the model group, Kw and KI were significantly elevated, while Bw was reduced drastically when compared with the normal group (P < 0.001, respectively, Table 2). Compared with the model group, the LDTPG, MDTPG, and HDTPG groups showed dramatic decreases in Kw and KI and a sharp increase in Bw (P < 0.05, respectively, Table 2); significant differences were observed in Kw, KI, and Bw among the LDTPG, MDTPG, and HDTPG groups (P < 0.05, respectively, Table 2).

3.4 Effects of TPG on pathomorphology of rat kidney tissue

The HE staining results showed that in the normal group, the renal tubules and glomeruli were morphologically normal, without any signs or symptoms of inflammatory cell infiltration, while the model group exhibited renal tubular swelling and congestion, degeneration, swelling, and vacuolar degeneration of kidney tissue cells, cell exfoliation in part of the epithelial layer, a thickening glomerular basement membrane, and massive inflammatory cell infiltration in the kidney tissue. Amelioration of the tubular and glomerular structures were noted in the intervention groups, especially the HDTPG group, when compared with the model group. See Figure 1.

3.5 Effects of TPG on glomerular ultrastructure

Compared with the normal group, the model group experienced endolysis within the tubular epithelium, breakage

Table 1. FBG, TG, TC and HDL-C levels in serum of difference groups (Mean±SD, n=9, mmol/L).

Group	Dose	FBG	TG	TC	HDL-C
Normal		5.12 ± 0.50	0.33 ± 0.04	55.82 ± 1.88	1.05 ± 0.07
Model		23.34 ± 1.70***	0.57 ± 0.03***	94.99 ± 1.43***	0.69 ± 0.05***
Low	1 mg/kg	19.98 ± 2.81#	0.56 ± 0.03#	84.87 ± 175#	0.81 ± 0.05#
Middle	2 mg/kg	13.70 ± 2.61##,$	0.48 ± 0.03##,$	72.48 ± 1.76##,$	0.83 ± 0.04##,$
High	8 mg/kg	9.23 ± 1.80###,$$,&	0.41 ± 0.02###,$$,&	68.91 ± 1.21###,$$,&	0.91 ± 0.04###,$$,&

FBG: Fasting blood glucose; TG: Triacylglycerol; TC: Total cholesterol; HDL-C: High density lipoprotein-cholesterol; ***: P < 0.001, compared with Normal; #: P < 0.05, ##: P < 0.01; ###:P < 0.001, compared with Model; $: P < 0.05; $$: P < 0.01, compared with Low; &: P < 0.05, compared with Middle.

Table 2. Urinary metabolic index level, renal weight, body weight and renal weight index in each group (Mean ± SD, n = 9).

Group	Dose	BUN (mmol/L)	Scr (μmol/L)	24 h Urine protein (mg)	Kidney wight (mg)	Body weight (kg)	KI (mg/kg)
Normal		5.75 ± 0.03	31.49 ± 1.79	10.59 ± 1.46	1.46 ± 0.22	0.36 ± 0.02	4.08 ± 0.61
Model		18.87 ± 2.29***	52.71 ± 1.53***	65.59 ± 4.06***	2.45 ± 0.25***	0.28 ± 0.02***	8.89 ± 0.94***
Low	1 mg/kg	16.52 ± 1.68#	40.37 ± 2.09#	52.62 ± 3.28#	2.11 ± 0.20#	0.27 ± 0.01#	7.77 ± 0.90#
Middle	2 mg/kg	14.00 ± 2.11##,$	36.87 ± 1.90##,$	42.41 ± 3.98##,$	1.95 ± 0.14##,$	0.32 ± 0.03##,$	6.03 ± 0.67##,$
High	8 mg/kg	13.29 ± 2.45###,$$,&	34.71 ± 1.61###,$$,&	40.36 ± 1.76###,$$,&	1.71 ± 0.15###,$$,&	0.34 ± 0.02###,$$,&	5.15 ± 0.67###,$$,&

***: P < 0.001, compared with Normal; #: P < 0.05; ##: P < 0.01; ###:P<0.001, compared with Model; $: P<0.05; $$: P<0.01, compared with Low; &: P < 0.05, compared with Middle

of the inner folded membrane, endothelial swelling within the glomerular capillaries, heterogeneity of the glomerular basement membrane, and partial foot process fusion; the LDTPG, MDTPG, and HDTPG groups saw varying degrees of improvement in the morphology of tubular epithelial cells and endothelial swelling within the glomerular capillaries, which was most pronounced in the HDTPG group. See Figure 2.

3.6 Intergroup comparison of PI3K/Akt signaling pathway-associated protein expression in kidney tissue

Comparing the model group with the normal group, PTEN protein expression was significantly reduced, PI3K protein expression was markedly elevated, and p-Akt/Akt was highly phosphorylated in the rat kidney tissue ($P < 0.001$, respectively,
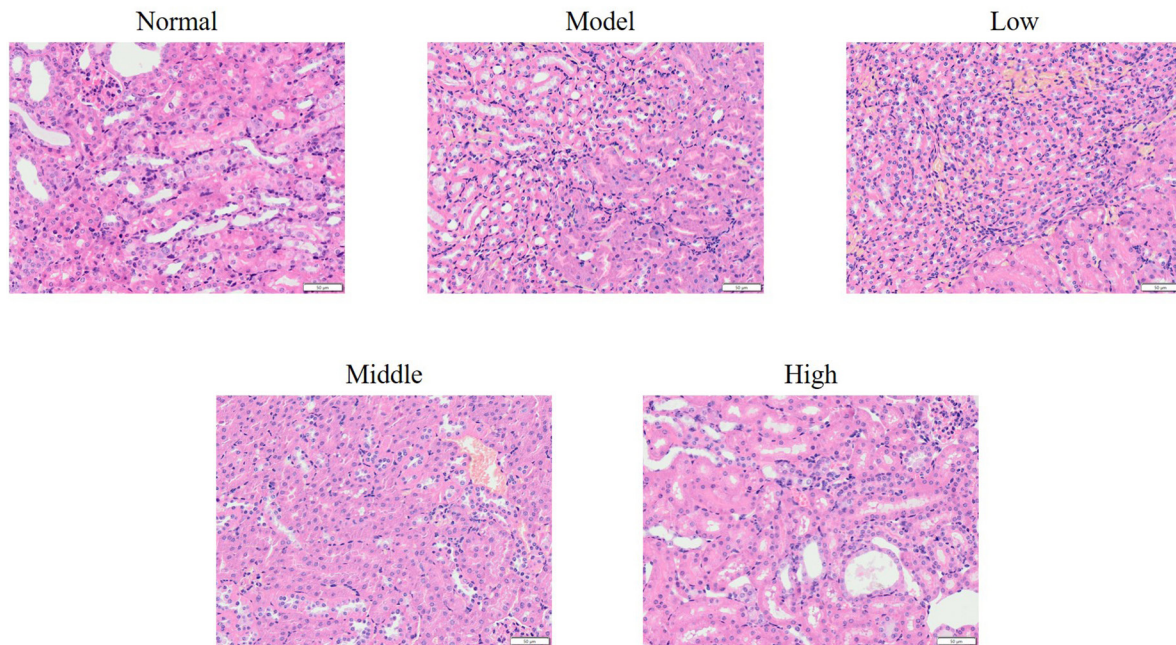

Figure 1. Observe the pathomorphological changes of renal tissue by HE staining (200×). Normal: The normal control group; Model: Diabetic induced kidney injury model group; Low: Model rats treated with 1mg/kg TG; Middle: The Model rats treated with 2 mg/kg TG; High: The Model rats treated with 8 mg/kg TG.
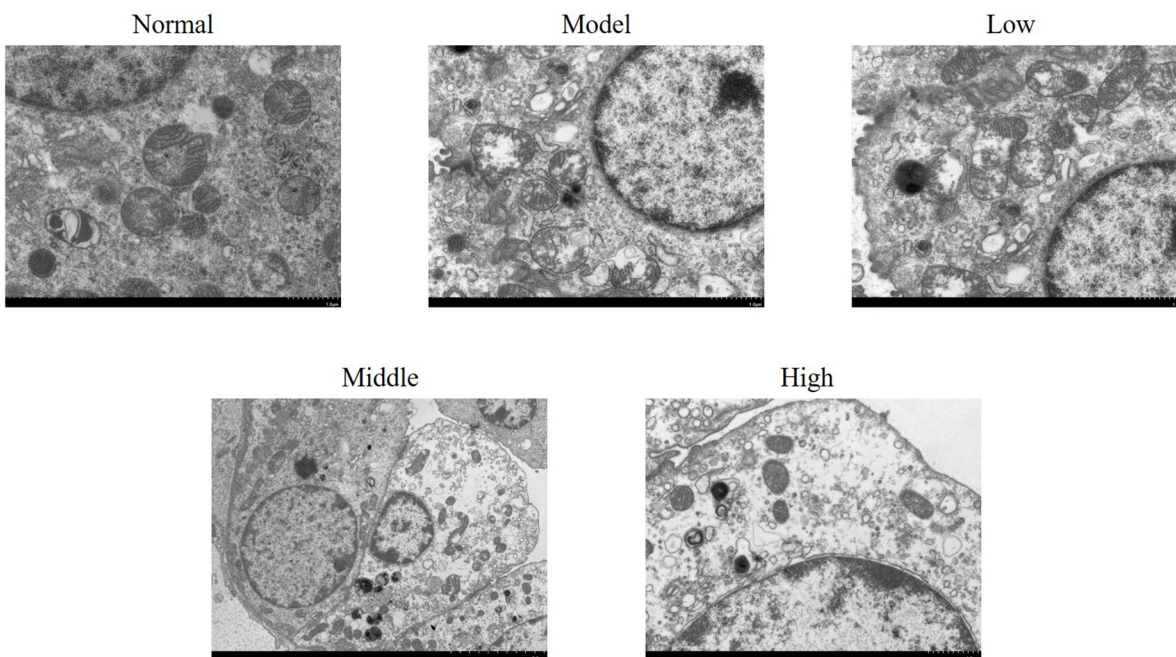

Figure 2. The ultrastructure of rat kidney was observed by transmission electron microscope (10000×). Normal: The normal control group; Model: Diabetic induced kidney injury model group; Low: Model rats treated with 1mg/kg TG; Middle: The Model rats treated with 2 mg/kg TG; High: The Model rats treated with 8 mg/kg TG

Figure 3); compared with the model group, the LDTPG, MDTPG, and HDTPG groups showed a considerable increase in PTEN protein expression and dramatic decreases in PI3K protein and phosphorylated p-Akt/Akt expression (P < 0.05, respectively, Figure 3), and the differences among the three groups were statistically significant (P < 0.05, respectively, Figure 3).

3.7 Effects of TPG on cell apoptosis in rat kidney tissue

Apoptotic cells were significantly increased in the model group as compared with the normal group (P < 0.001, Figure 4) and were drastically reduced in the LDTPG, MDTPG, and HDTPG groups in comparison with the model group (P < 0.05, respectively, Figure 4), with the differences among the LDTPG,

MDTPG, and HDTPG groups suggesting statistical significance (P < 0.05, respectively, Figure 4).

3.8 Effects of TPG on apoptosis-associated protein (Bcl-2, Bax, caspase-3) expression in rat kidney tissue

Compared with the normal group, the model group showed that Bcl-2 protein expression was markedly reduced, and Bax and caspase-3 protein expression were vastly elevated in the rat kidney tissue (P < 0.001, respectively, Figure 5); the LDTPG, MDTPG, and HDTPG groups exhibited considerably increased Bcl-2 protein expression and substantially reduced Bax and caspase-3 protein expression as compared with the model group,
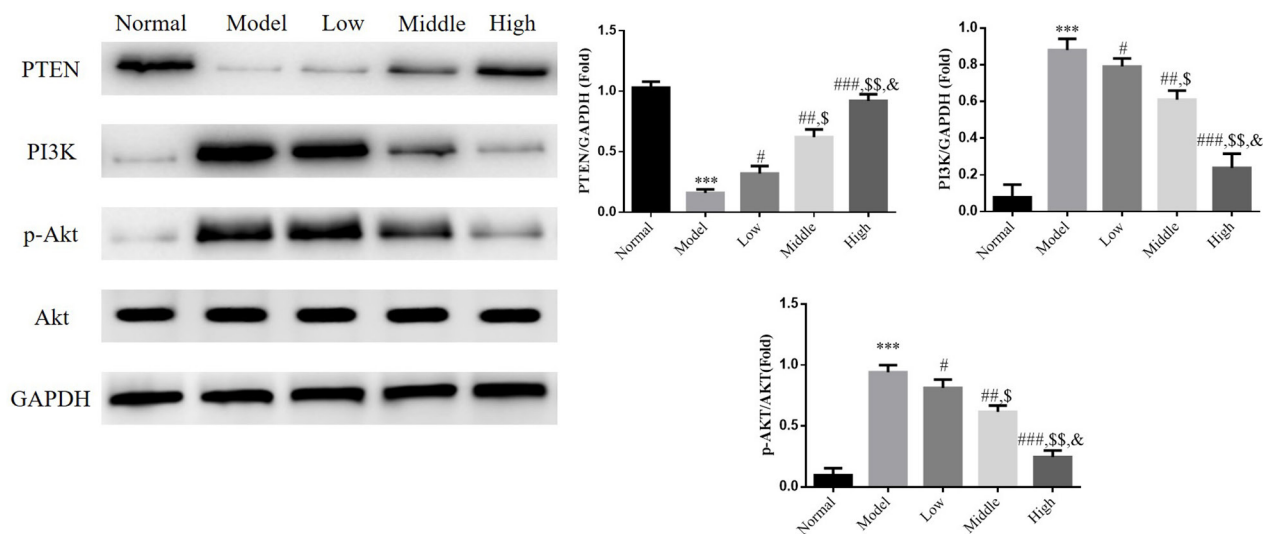

Figure 3. PTEN, PI3K, p-Akt protein expression by WB assay. Normal: The normal control group; Model: Diabetic induced kidney injury model group; Low: Model rats treated with 1mg/kg TG; Middle: The Model rats treated with 2 mg/kg TG; High: The Model rats treated with 8 mg/kg TG. ***: P < 0.001, vs. Normal; #: P < 0.05, ##: P < 0.01, ###: P < 0.001, vs. Model; $: P < 0.05, $$: P < 0.01, vs. Middle; &: P < 0.05, vs. Middle.

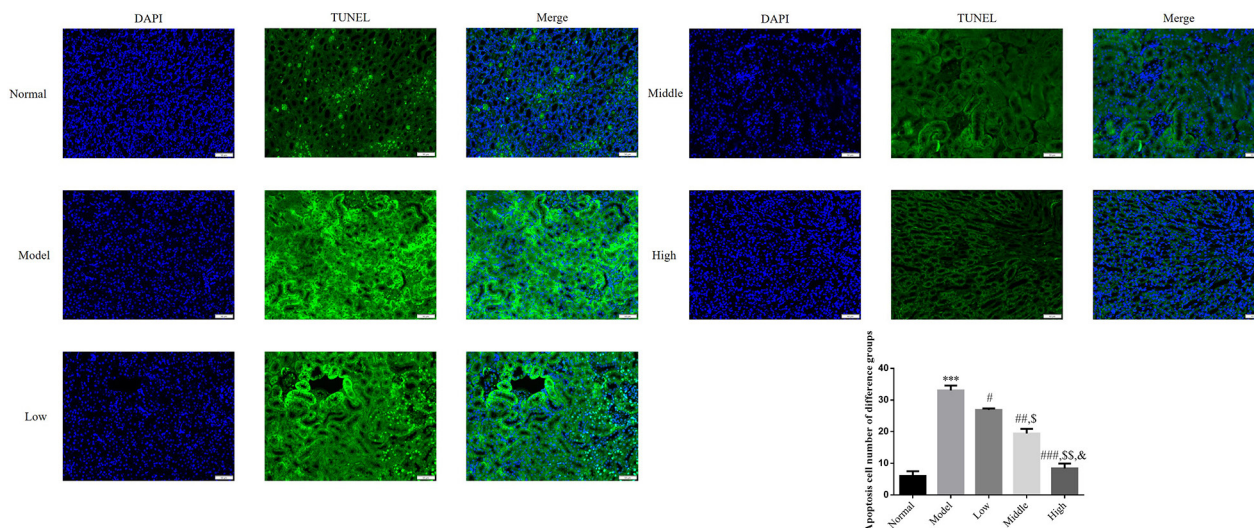**Figure 4**. Observed apoptosis cell by TUNEL in kidney tissues (200×). Normal: The normal control group; Model: Diabetic induced kidney injury model group; Low: Model rats treated with 1mg/kg TG; Middle: The Model rats treated with 2 mg/kg TG; High: The Model rats treated with 8 mg/kg TG. ***: P < 0.001, vs. Normal; #: P < 0.05, ##: P < 0.01, ###: P < 0.001, vs. Model; $: P < 0.05, $$: P < 0.01, vs. Middle; &: P < 0.05, vs. Middle.
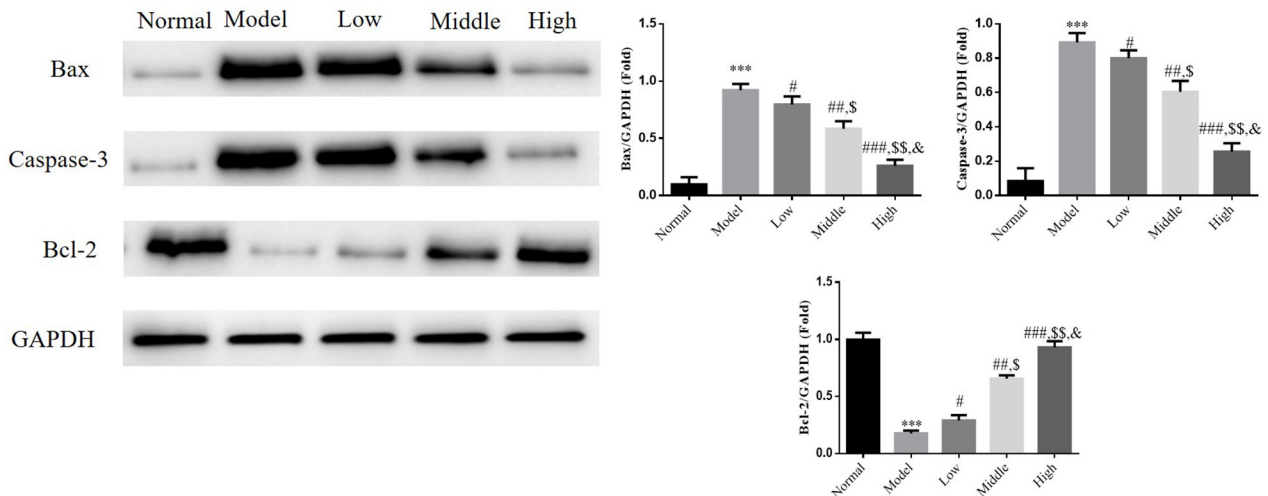
Figure 5. Bax, Caspase-3 and Bcl-2 protein expression in kidney tissues. Normal: The normal control group; Model: Diabetic induced kidney injury model group; Low: Model rats treated with 1mg/kg TG; Middle: The Model rats treated with 2 mg/kg TG; High: The Model rats treated with 8 mg/kg TG. ***: P < 0.001, vs. Normal; #: P < 0.05, ##: P < 0.01, ###: P < 0.001, vs. Model; $: P < 0.05, $$: P < 0.01, vs. Middle; &: P < 0.05, vs. Middle.

and the differences among the three groups were statistically significant (P < 0.05, respectively, Figure 5).

4 Discussion

Diabetic nephropathy is glomerulosclerosis caused by hyperglycemia attributed to the metabolic changes of diabetes, which often presents with impaired kidney function (e.g., hematuria, albuminuria) and is pathologically manifested as glomerular basement membrane damage, epithelial cell degeneration in the kidney tissue, tubular injury, and even kidney failure when it reaches the advanced stage – a major cause of death for patients with diabetes. The results of this study confirmed the occurrence of renal edema and functional impairment. According to the histological and TEM findings, the diabetic rats suffered from tubular injury (e.g., swelling, congestion), endolysis within the tubular epithelium, breakage of the inner folded membrane, endothelial swelling within the glomerular capillaries, heterogeneity of the glomerular basement membrane, and partial foot process fusion, which conformed to the modeling results of preceding studies (Tu et al., 2019; Tang et al., 2020; Chen et al., 2019) and further demonstrated the presence of kidney injury in the diabetic rats and the establishment of the rat model of diabetes-induced kidney injury. From the results of this study, it was noted that TPG offered kidney protection to diabetic rats by alleviating renal edema and kidney tissue injury.

The PI3K/Akt signaling pathway plays a crucial role in the intracellular transduction of membrane receptor signals and cell proliferation, differentiation, and apoptosis. It has been recently reported that overactivation of the PI3K/Akt signaling pathway is strongly associated with the development and progression of diabetic nephropathy (Cui et al., 2019; Liang et al., 2019; Chen et al., 2020). PTEN is a negative regulator of the PI3K/Akt upstream signaling pathway involved in the development of diabetic nephropathy (Haddadi et al., 2018; Liu et al., 2019; Maidarti et al., 2020). PTEN, as an active player in the development of a range of diseases, deactivates the PI3K substrate to reduce

the PI3K level and block downstream Akt phosphorylation (Carnero & Paramio, 2014). Huang et al. (2017) discovered that upon activation, the PI3K/Akt signaling pathway could mediate podocyte injury. Lu et al. (2016) noted that reduced PTEN protein expression could mediate TGF-β1 to trigger overactivation of the PI3K/Akt signaling pathway and thereby promote glomerular epithelial-to-mesenchymal transition. This study suggested that the negative regulation of the PIK3/Akt signaling pathway by PTEN was probably involved in the development of diabetes-induced kidney injury. Elevated PTEN expression and reduced PI3K protein and phosphorylated Akt expression were observed in the TPG-treated kidney tissue, suggesting the inhibitory role of TPG in the activation of the PI3K/Akt signaling pathway to ameliorate kidney tissue injury and impaired kidney function.

With apoptosis being an important pathogenesis of diabetic nephropathy, the decline in cell counts in the kidney tissue might be explained by cell apoptosis in the process of glomerulosclerosis (Tsai et al., 2018). Caspase-3 is recognized as the most important protease for cell apoptosis and downstream effector involved in multiple apoptotic pathways for initiation and execution of apoptosis (Olivera Santa-Catalina et al., 2017). Reportedly, phosphorylated Akt acts on downstream Bcl-2 and caspase-3 via the activated PI3K/Akt signaling pathway to mediate cell proliferation and apoptosis (Ma et al.,2018). This study revealed the protective and anti-apoptotic activities of TPG against kidney injury, which was closely associated with the PIK3/Akt/caspase-3 signaling cascade.

In conclusion, TPG suppresses the activation of the PI3K/Akt signaling pathway to alleviate kidney injury in diabetic rats, reduce apoptotic cells in kidney tissue and thereby mediate tissue repair and functional recovery. This new finding about the therapeutic effect of TPG hopefully can provide a reference for the treatment of diabetic nephropathy. Despite all that, this study still has its own limitations: TPG cannot completely reverse but alleviate diabetes-induced kidney injury probably because

TPG has an association with other pathways. Therefore, further study is needed to elucidate the underlying mechanism of action.

References

Carnero, A., & Paramio, J. M. (2014). The PTEN/PI3K/AKT pathway in vivo, cancer mouse models. *Frontiers in Oncology*, 4, 252. http://dx.doi.org/10.3389/fonc.2014.00252. PMid:25295225.

Chen, J., Wang, X., He, Q., Bulus, N., Fogo, A. B., Zhang, M. Z., & Harris, R. C. (2020). YAP activation in renal proximal tubule cells drives diabetic renal interstitial fibrogenesis. *Diabetes*, 69(11), 2446-2457. http://dx.doi.org/10.2337/db20-0579. PMid:32843569.

Chen, Y.-J., Kong, L., Tang, Z.-Z., Zhang, Y.-M., Liu, Y., Wang, T.-Y., & Liu, Y.-W. (2019). Hesperetin ameliorates diabetic nephropathy in rats by activating Nrf2/ARE/glyoxalase 1 pathway. *Biomedicine and Pharmacotherapy*, 111, 1166-1175. http://dx.doi.org/10.1016/j.biopha.2019.01.030. PMid:30841430.

Cui, F.-Q., Wang, Y.-F., Gao, Y.-B., Meng, Y., Cai, Z., Shen, C., Liu, Z.-Q., Jiang, X.-C., & Zhao, W.-J. (2019). Effects of BSF on podocyte apoptosis via regulating the ROS-Mediated PI3K/AKT Pathway in DN. *Journal of Diabetes Research*, 2019, 9512406. http://dx.doi.org/10.1155/2019/9512406. PMid:31886291.

Giugliano, D., Longo, M., Scappaticcio, L., Caruso, P., & Esposito, K. (2021). Sodium-glucose transporter-2 inhibitors for prevention and treatment of cardiorenal complications of type 2 diabetes. *Cardiovascular Diabetology*, 20(1), 17. http://dx.doi.org/10.1186/s12933-021-01213-w. PMid:33430860.

Haddadi, N., Lin, Y., Travis, G., Simpson, A. M., Nassif, N. T., & McGowan, E. M. (2018). PTEN/PTENP1: 'Regulating the regulator of RTK-dependent PI3K/Akt signalling', new targets for cancer therapy. *Molecular Cancer*, 17(1), 37. http://dx.doi.org/10.1186/s12943-018-0803-3. PMid:29455665.

Huang, G., Zou, B., Lv, J., Li, T., Huai, G., Xiang, S., Lu, S., Luo, H., Zhang, Y., Jin, Y., & Wang, Y. (2017). Notoginsenoside R1 attenuates glucose induced podocyte injury via the inhibition of apoptosis and the activation of autophagy through the PI3K/ Akt/ mTOR signaling pathway. *International Journal of Molecular Medicine*, 39(3), 559-568. http://dx.doi.org/10.3892/ijmm.2017.2864. PMid:28112381.

Izzo, A., Massimino, E., Riccardi, G., & Della Pepa, G. (2021). A narrative review on sarcopenia in Type 2 Diabetes Mellitus: prevalence and associated factors. *Nutrients*, 13(1), 183. http://dx.doi.org/10.3390/nu13010183. PMid:33435310.

Jablonski, P., Howden, B. O., Rae, D. A., Birrell, C. S., Marshall, V. C., & Tange, J. (1983). An experimental model for assessment of renal recovery from warm ischemia. *Transplantation*, 35(3), 198-204. http://dx.doi.org/10.1097/00007890-198303000-00002. PMid:6340272.

Lei, X., Zhang, L., Li, Z., & Ren, J. (2018). Astragaloside IV/lncRNA-TUG1/TRAF5 signaling pathway participates in podocyte apoptosis of diabetic nephropathy rats. *Drug Design, Development and Therapy*, 12, 2785-2793. http://dx.doi.org/10.2147/DDDT.S166525. PMid:30233141.

Liang, F., Ren, C., Wang, J., Wang, S., Yang, L., Han, X., Chen, Y., Tong, G., & Yang, G. (2019). The crosstalk between STAT3 and p53/RAS signaling controls cancer cell metastasis and cisplatin resistance via the Slug/MAPK/PI3K/AKT-mediated regulation of EMT and autophagy. *Oncogenesis*, 8(10), 59. http://dx.doi.org/10.1038/s41389-019-0165-8. PMid:31597912.

Liu, H.-Y., Zhang, Y.-Y., Zhu, B.-L., Feng, F.-Z., Yan, H., Zhang, H.-Y., & Zhou, B. (2019). miR-21 regulates the proliferation and apoptosis of ovarian cancer cells through PTEN/PI3K/AKT. *European Review for Medical and Pharmacological Sciences*, 23(10), 4149-4155. PMid:31173285.

Lu, H., Chen, B., Hong, W., Liang, Y., & Bai, Y. (2016). TGF-β1 stimulates hedgehog signalling to promote epithelial-mesenchymal transition after kidney injury. *FEBS Journal*, 283(20), 3771-3378. http://dx.doi.org/10.1111/febs.13842.

Lu, Q., Wang, W.-W., Zhang, M.-Z., Ma, Z.-X., Qiu, X.-R., Shen, M., & Yin, X.-X. (2019). ROS induces epithelial-mesenchymal transition via the TGF-β1/ PI3K/ Akt/ mTOR pathway in diabetic nephropathy. *Experimental and Therapeutic Medicine*, 17(1), 835-846. PMid:30651870.

Ma, R., Zhao, L.-N., Yang, H., Wang, Y.-F., Hu, J., Zang, J., Mao, J.-G., Xiao, J.-J., & Shi, M. (2018). RNA binding motif protein 3 (RBM3) drives radioresistance in nasopharyngeal carcinoma by reducing apoptosis via the PI3K/ AKT/ Bcl-2 signaling pathway. *American Journal of Translational Research*, 10(12), 4130-4140. PMid:30662656.

Maidarti, M., Anderson, R. A., & Telfer, E. E. (2020). Crosstalk between PTEN/PI3K/Akt signalling and DNA damage in the oocyte: implications for primordial follicle activation, oocyte quality and ageing. *Cells*, 9(1), 200. http://dx.doi.org/10.3390/cells9010200. PMid:31947601.

Malik, S., Suchal, K., Khan, S. I., Bhatia, J., Kishore, K., Dinda, A. K., & Arya, D. S. (2017). Apigenin ameliorates streptozotocin-induced diabetic nephropathy in rats via MAPK-NF-kappaB-TNF-alpha and TGF-beta1-MAPK-fibronectin pathways. *American Journal of Physiology. Renal Physiology*, 313(2), F414-F422. http://dx.doi.org/10.1152/ajprenal.00393.2016. PMid:28566504.

Olivera Santa-Catalina, M., Caballero Bermejo, M., Argent, R., Alonso, J. C., Centeno, F., & Lorenzo, M. J. (2017). JNK signaling pathway regulates sorbitol-induced Tau proteolysis and apoptosis in SH-SY5Y cells by targeting caspase-3. *Archives of Biochemistry and Biophysics*, 636, 42-49. http://dx.doi.org/10.1016/j.abb.2017.11.004. PMid:29126968.

Su, X., Feng, X., Terrando, N., Yan, Y., Chawla, A., Koch, L. G., Britton, S. L., Matthay, M. A., & Maze, M. (2013). Dysfunction of inflammation-resolving pathways is associated with exaggerated postoperative cognitive decline in a rat model of the metabolic syndrome. *Molecular Medicine (Cambridge, Mass.)*, 18(12), 1481-1490. http://dx.doi.org/10.2119/molmed.2012.00351. PMid:23296426.

Tang, L., Li, K., Zhang, Y., Li, H., Li, A., Xu, Y., & Wei, B. (2020). Quercetin liposomes ameliorate streptozotocin-induced diabetic nephropathy in diabetic rats. *Scientific Reports*, 10(1), 2440. http://dx.doi.org/10.1038/s41598-020-59411-7. PMid:32051470.

Tsai, Y.-C., Kuo, P.-L., Hung, W.-W., Wu, L.-Y., Wu, P.-H., Chang, W.-A., Kuo, M.-C., & Hsu, Y.-L. (2018). Angpt2 induces mesangial cell apoptosis through the MicroRNA-33-5p-SOCS5 loop in diabetic nephropathy. *Molecular Therapy. Nucleic Acids*, 13, 543-555. http://dx.doi.org/10.1016/j.omtn.2018.10.003. PMid:30414568.

Tu, Q., Li, Y., Jin, J., Jiang, X., Ren, Y., & He, Q. (2019). Curcumin alleviates diabetic nephropathy via inhibiting podocyte mesenchymal transdifferentiation and inducing autophagy in rats and MPC5 cells. *Pharmaceutical Biology*, 57(1), 778-786. http://dx.doi.org/10.1080/13880209.2019.1688843. PMid:31741405.

Wan, L., Liu, J., Huang, C. B., Wang, Y., Lei, L., Liu, L., Cheng, Y. Y., & Feng, Y. X. (2013). Effect of tripterygium glycosides on pulmonary function in adjuvant arthritis rats. *Journal of the Chinese Medical Association*, 76(12), 715-723. http://dx.doi.org/10.1016/j.jcma.2013.08.002. PMid:24060529.

Xing, L., Liu, Q., Fu, S., Li, S., Yang, L., Liu, S., Hao, J., Yu, L., & Duan, H. (2015). PTEN inhibits high glucose-induced phenotypic transition in podocytes. *Journal of Cellular Biochemistry*, 116(8), 1776-1784. http://dx.doi.org/10.1002/jcb.25136. PMid:25736988.